J MATER SCI 41 (2006) 3645–3655

Monitoring the fracture of wood in torsion using acoustic emission

ZHENG CHEN*, BRIAN GABBITAS, DAVID HUNT
University of New Brunswick, Canada

Published online: 21 April 2006

Acoustic emission (AE) was used to monitor the failure process of hardwood and softwood test-pieces under static and fatigue torsional loading. In static torsional-loading tests, acoustic activity indicated some microcrack initiation before the visible cracking in both hardwood and softwood test-pieces. Hardwood produced more AE counts than softwood during testing, and the grain angle of test-pieces influenced the total AE counts. During torsional fatigue fracture, increased acoustic activity indicated the onset of microcrack formation. Fatigued test-pieces produced more total AE counts during fracture than static test-pieces, provided the angle of twist exceeded a minimum value. The results show that it is possible to monitor and analyze the failure process in wood when under torsional loading using acoustic emission techniques.

1. Introduction

Acoustic emission (AE) is a widely used non-destructive technique for characterizing damage evolution during loading in various materials. It is defined as a transient elastic wave generated by the rapid release of energy within a material. The information about the AE technique is widely documented [1–6]. Bucur [7] has given the principles and a literature review of the AE technique in her 1995 publication on the acoustics of wood. Since crack nucleation and growth results in a sudden change of energy within a material, acoustic emission can be used as an analytical tool for monitoring crack nucleation and growth.

Studies of wood using acoustic emission have increased over the past twenty years. Recently there have been two areas of interest where AE has been used to study cracking in wood. Firstly there has been interest in the possibility of using acoustic emission to monitor and control the drying of wood in order to eliminate or minimize drying defects [8–10]. However, the variability between different types of wood, such as differences in earlywood to latewood ratio and differences in inherent defects within the same species (the anisotropy, heterogeneity, and the presence of natural defects in wood, etc.), has so far inhibited any practical application. Nevertheless, Kowalski *et al*. [11] found three characteristic groups of acoustic signals in birch wood samples during drying and explained them using a mechanistic model of drying. They commented that during drying the on-line observations of the development of acoustic events when cracking occurs at different drying stages is important. Secondly acoustic emission has been used to monitor fracture behaviour in wood during the application of various types of applied loading. Ansell [12] has studied the behaviour of three softwoods under tensile loading and found that the shape of the AE-strain curve was influenced by the earlywood to latewood ratio. Schniewind *et al*. [13] collected AE signals during mode I and mixed mode tests at different moisture contents and temperatures. They found that the AE activity in mixed mode tests was much higher than that for mode I. Aicher *et al*. [14] used AE to localize crack nucleation in glulam loaded in tension perpendicular to grain. Dill-Langer and Aicher [15] used AE technology to monitor the fracture of clear spruce wood under tensile loading. They found that there was an on-set of AE prior to the first visible crack growth step. Using acoustic emission to monitor mode I fracture of softwoods (spruce and pine) and hardwoods (alder, oak and ash), Reiterer *et al*. [16] stated that the AE counts up to maximum force are much higher for the softwoods. This supports the idea that softwoods build a process zone containing more micro cracks. The differences in macrocrack formation and propagation are visible in the shape of the cumulative AE counts. Kánnár [17] defined that for the Kaiser effect of wood [18], it is the acceptance of the decreasing effect of acoustic activity in the first loading cycle, when the events obtained during later loading cycles are fewer than 50% of those in the first loading cycle. Kánnár [17] reported that 90%

*Author to whom all correspondence should be addressed.
0022-2461
DOI: 10.1007/s10853-006-6292-6

of Scots pine, when tested under tension in the *LR* plane, shows the Kaiser effect in the second loading cycle immediately following the previous load. However, the greater the elapsed time until the second loading period, the less the effect can be observed. Also significant changes in moisture content and temperature can result in the disappearance of the Kaiser effect.

There is little reported work in the literature for studies on wood under either static or fatigue torsional loading conditions using the AE technique. The failure mode of wood in torsion under static or fatigue loading is more complicated than tension or pure shear loading [19]. Although torsional loading is not perceived to be of general importance, in some applications where flexure is dominant, there may also be some twisting. For example, the blades in a wind turbine would be subjected to torsional as well as flexural loading. In order to investigate failure in shear under torsional loading in softwood and hardwood, an AE technique has been used to monitor the fracture of wood under torsional loading as the part of a larger programme which investigated the torsional fatigue characteristics of wood [19].

2. Materials and methods

2.1. Test pieces

The hardwood (Red Lauan) and softwood (Sitka Spruce) with different grain orientations were used for the test pieces. The test pieces were solid cylinders 220 mm long with a 20 mm diameter cross section and with square expanded ends. Angle of twist measurements were taken over a 120 mm length using a calibrated strain gauge transducer (Fig. 1).

2.2. Torsional fatigue experiments

A Mayes servo-hydraulic tensile testing machine was used for the torsional fatigue testing (Fig. 2a). An attachment to the testing machine for transferring the linear movement of the machine into rotational motion was designed and manufactured (Fig. 2b). The angle of twist was determined using a specially designed strain measuring transducer attached to the test piece (Fig. 1). All tests were carried out in displacement mode. In the static torsional test, the load speeds were set at 3-4 degrees of twist angle per second. In the torsional fatigue tests, the rate of load cycling was always less than 10 cycles per minute (0.17 Hz) under unidirectional (pulsating) load. Measurements of cyclic load, strain, cross-head movement and time were made during each test.

2.3. Acoustic emission

The equipment used for AE (acoustic emission) analysis was the Dunegan 3000 series detector. The AE signal was monitored by a 9201A transducer attached to the specimen by a tape with silicone liquid for transfer of emission. The signals were then passed into a pre-amplifier which boosted the signal (60 dB). A band-pass filter of 100–300 kHz eliminated any low frequency emission: the generated noise in the laboratory was thus eliminated and only the frequency range corresponding to optimum transducer efficiency was allowed to pass through. From the pre-amplifier, the signals were passed into the post-amplifier, which boosted the signals a further (20 dB), giving a total gain of 80 dB. In the case of ringdown counting, each AE peak above a given threshold (100 μv)

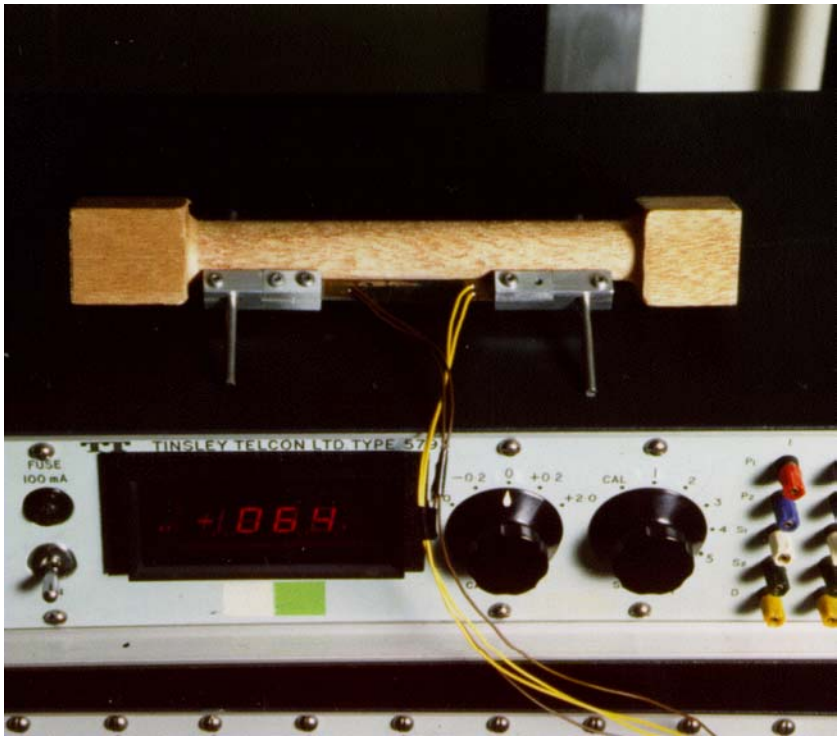

Figure 1 A torsion test-piece with strain transducers and instrumentation, for measuring the angle of twist, attached.

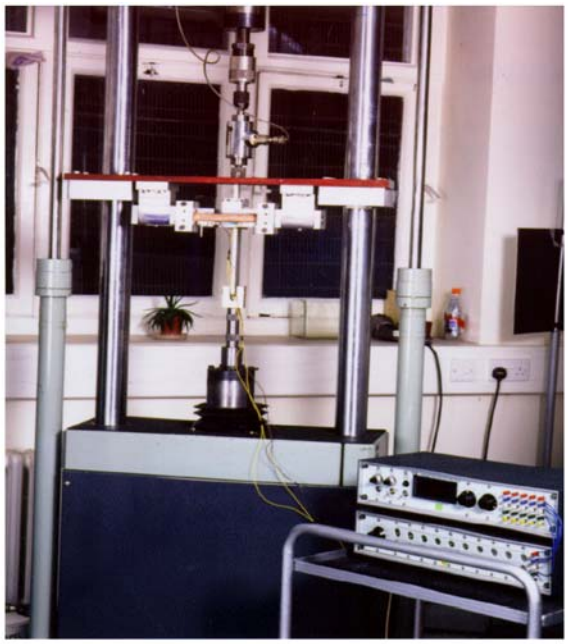

(a)

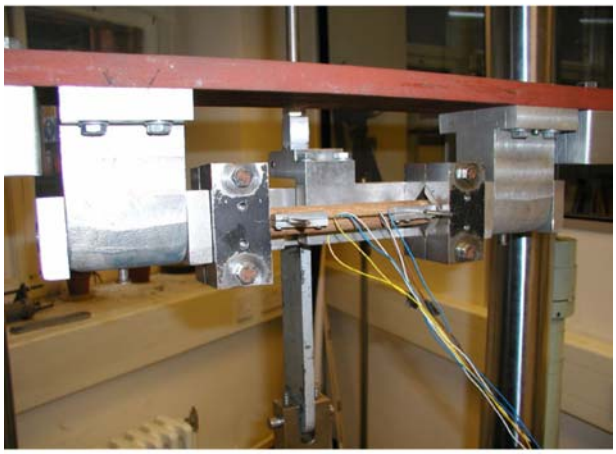

(b)

Figure 2 (a) A mayes tensile testing machine adapted to convert linear movement into rotational movement for torsional fatigue loading. (b) Detail of the torsional loading attachment.

was monitored on a digital counter and also displayed on a chart recorder and computer. Thus cumulative AE counts could be superimposed on to the load-time curves.

AE monitoring was carried out using module 303 for crack monitoring in static and fatigue torsion tests, and module 920 for comparison of acoustic emission in each cycle. Module 303 recorded total AE counts (cumulative events) in each 0.1 s. Module 920 was used to count the sum of events in each 0.1 s. In module 303 the gain was set to 55 dB and the rate of AE sample collection rate was at either 10 or 20 samples per second. In module 920, the amplifier mode was selected with a threshold of 25 dB and an envelope dead time was set at 1 μs. By connecting to a computer using a CIO-DAS0J8/Jr A/D card, the total AE counts per 0.05 second from module 303 or the sum of AE events per 0.05 sec from module 920 were recorded directly to Microsoft office files for calculation and plotting of total AE counts versus time.

3. Results and discussion

3.1. Crack monitoring in static torsion tests using acoustic emission

A series of hardwood and softwood test-pieces, with different grain angles, were tested at the same loading rate. The curves of total AE counts and shear stress versus time are given in Figs 3–8. Here Figs 3–5 are the curves for the hardwood test-pieces with grain angles at 0°, 45° and 90° respectively. Figs 6–8 are the curves for the softwood test-pieces with grain angles at 0°, 45° and 90° respectively. The results show that AE activity takes place before the maximum load. Fig. 9 shows the curves of total AE counts and shear stress versus time for a hardwood test-piece with a 0° grain angle that was loaded and the test stopped just before the maximum load was reached. Fig. 10 shows the curves of total AE counts and shear stress versus time for a softwood test-piece with a 0° grain angle that was loaded and the test stopped just before the maximum load was reached. The results shown in Figs 9–10 confirm that AE activity takes place before the maximum load (the results shown in Figs 3–8). The cross-sections of these samples were examined using optical microscopy (Figs 11–12). Microcracks were observed in the vicinity of a ray in the hardwood (Fig. 11) and in the softwood there were microcracks and cell deformation (Fig. 12). This suggests that the time from the onset of AE activity to maximum load is a period of microcrack formation.

Table I gives values for the ratio of the load at the onset of AE to the maximum load for different grain orientations in both the hardwood and the softwood. The data indicates that grain orientation in both hardwood and softwood influences the maximum torsional load and the torsional load at the onset of AE activity. With increasing grain angle both the ultimate torsional load, the torsional load at the onset of AE activity and the ratio of the load at AE onset to the maximum load decrease. This suggests that AE activity is more easily stimulated as the grain angle increases. Table I also shows the total AE counts when the applied torsional load reaches its maximum value. For the softwood and the hardwood, with a grain orientation at 45° to the twist axis, the total AE counts at maximum torsional loading are lower than for other grain orientations. The results suggest that for grain angles from 0° to 45°; the total AE counts at maximum loading decrease as the corresponding torsional strength of wood decreases, but for grain angles from 45° to 90°, the total AE counts at maximum loading increases as the torsional strength of wood decreases. As the grain orientation relative to the twist axis varies, there is a relation between grain angle and fracture mode for wood under torsional loading as shown in Table II [19]. For a 0° grain angle the fracture is Mode II_{RL} or Mode II_{RT}, but for a 45° grain orientation it changes to Mode I_{RL} and Mode I_{RT}. At 90° the fracture is

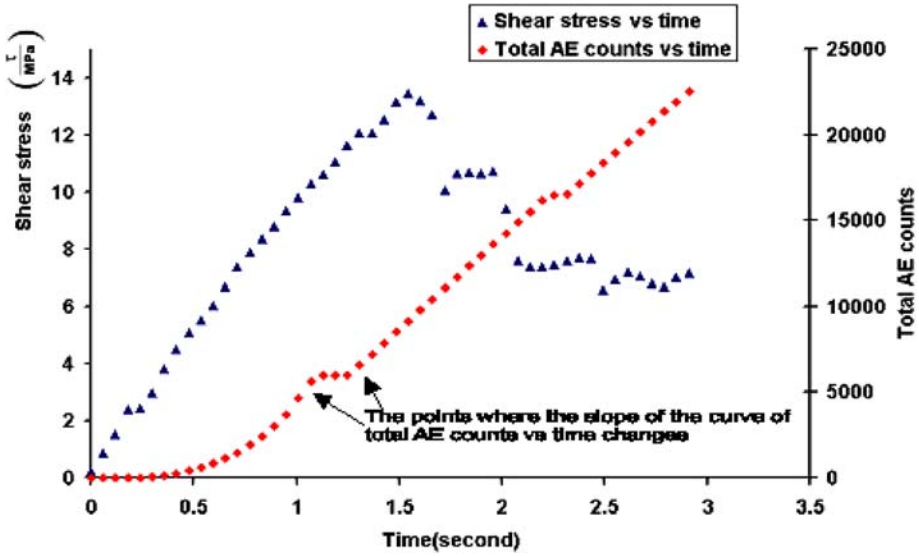

Figure 3 Total AE counts vs time compared with shear stress vs time for a hardwood having a 0° grain angle under static torsional loading. Module 303 has been used.

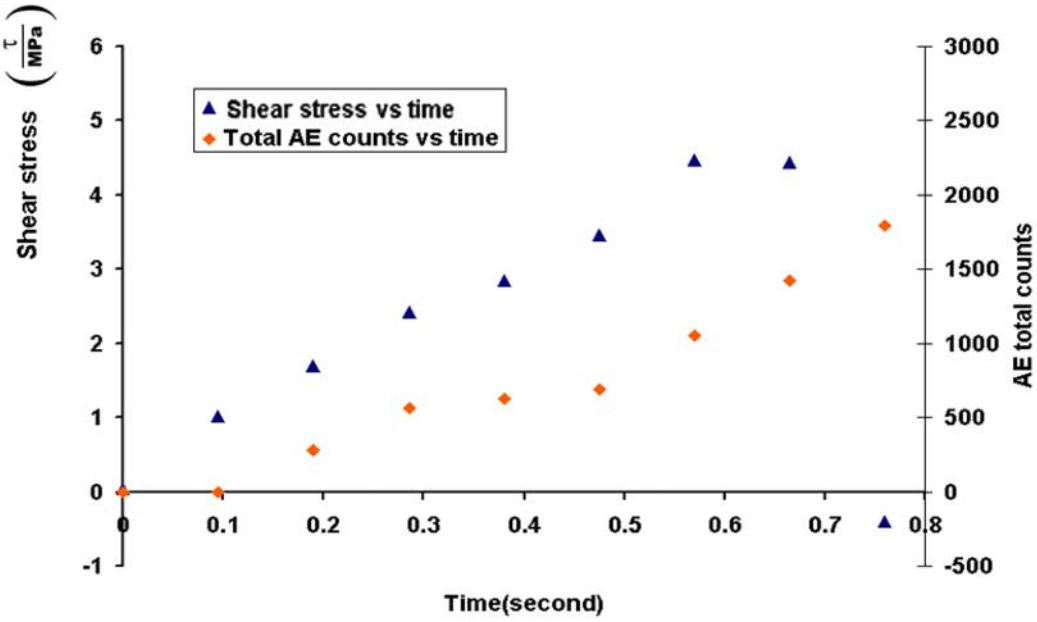

Figure 4 Total AE counts vs time compared with shear stress vs time for a hardwood having a 45° grain angle under static torsional loading. Module 303 has been used.

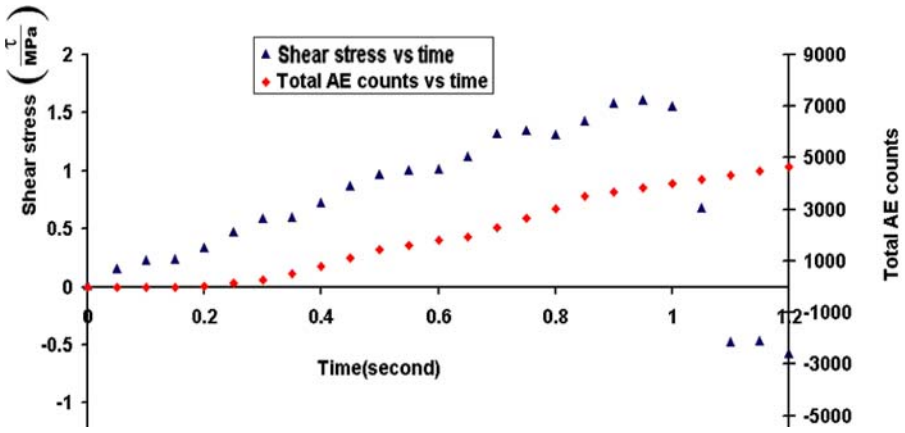

Figure 5 Total AE counts vs time compared with shear stress vs time for a hardwood having a 90° grain angle under static torsional loading. Module 303 has been used.

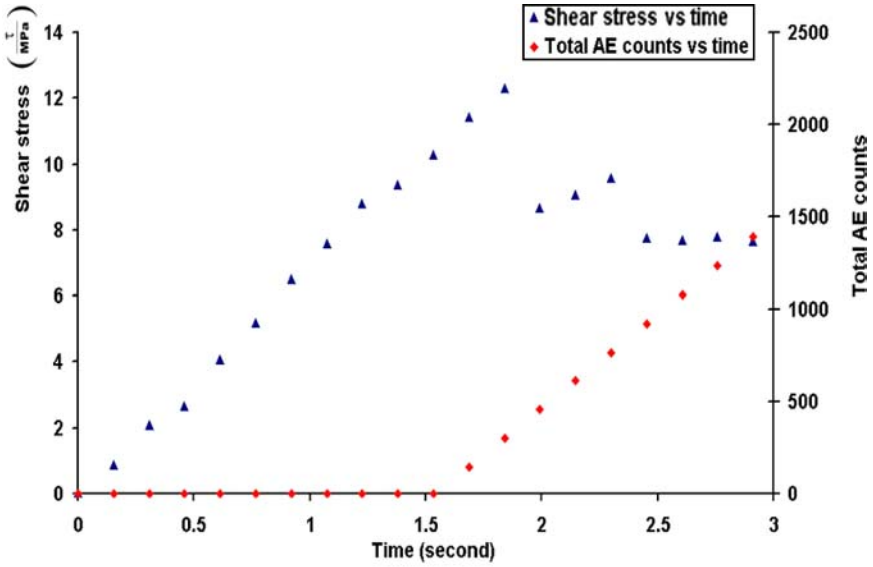

Figure 6 Total AE counts vs time compared with shear stress vs time for a softwood having a 45° grain angle under static torsional loading. Module 303 has been used.

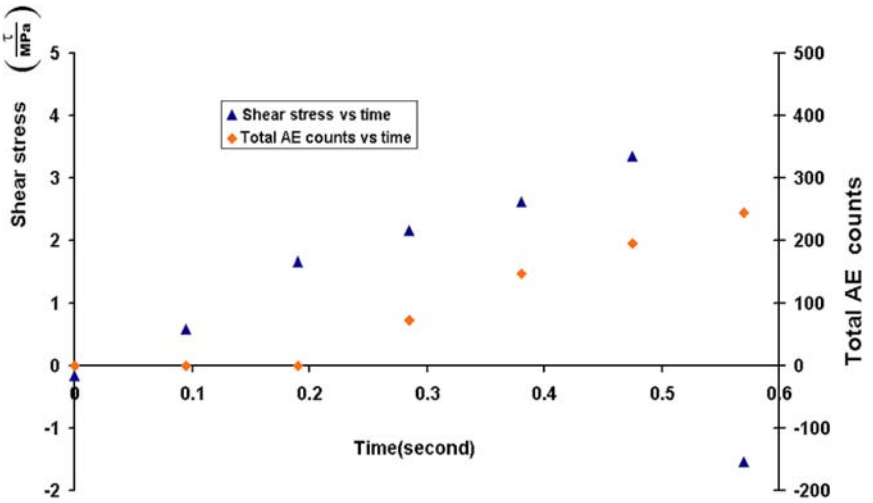

Figure 7 Total AE counts vs time compared with shear stress vs time for a softwood having a 45° grain angle under static torsional loading. Module 303 has been used.

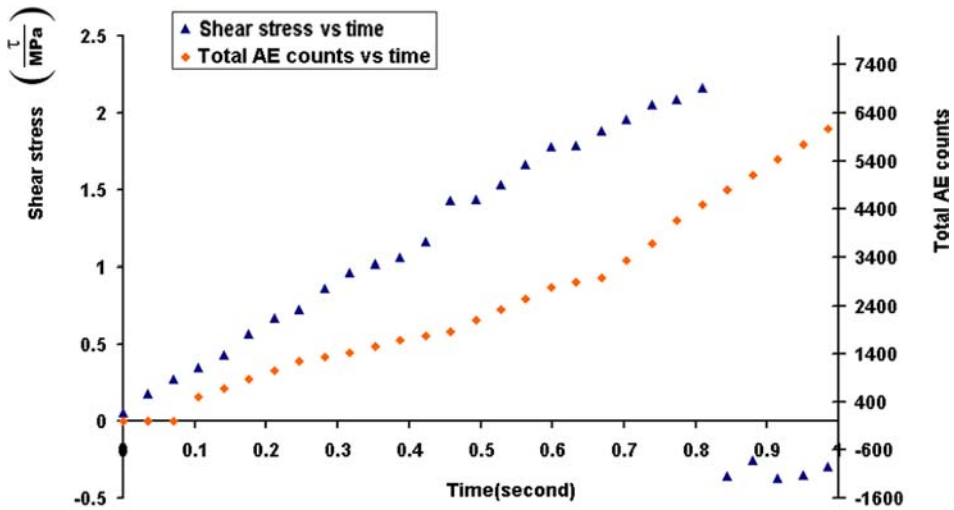

Figure 8 Total AE counts vs time compared with shear stress vs time for a softwood having a 90° grain angle under static torsional loading. Module 303 has been used.

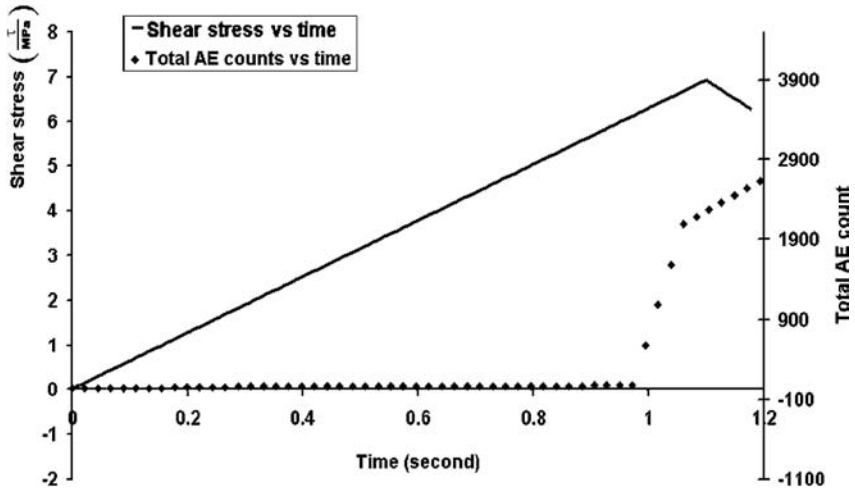

Figure 9 Total AE counts vs time compared with shear stress vs time for a hardwood with a 0° grain angle under static torsional loading. The test was stopped just before the maximum load was reached. Module 303 has been used.

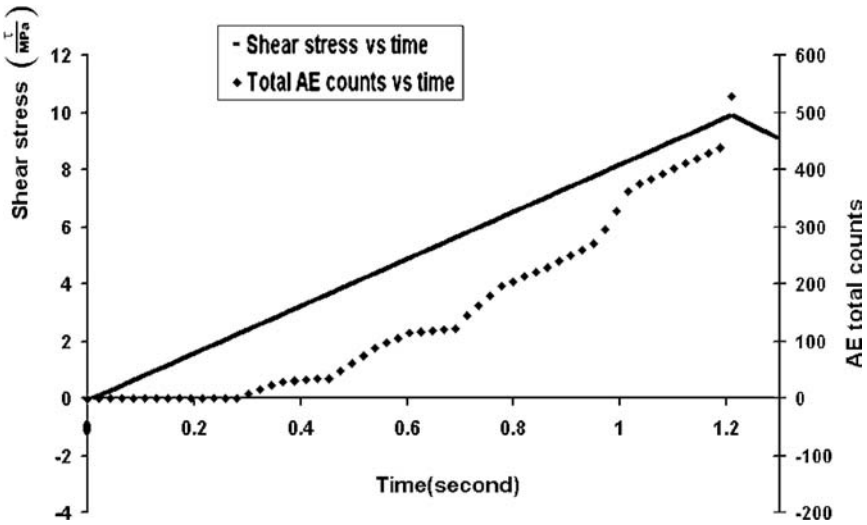

Figure 10 Total AE counts vs time compared with shear stress vs time for a softwood with a 0° grain angle under static torsional loading. The test was stopped just before the maximum load was reached. Module 303 has been used.

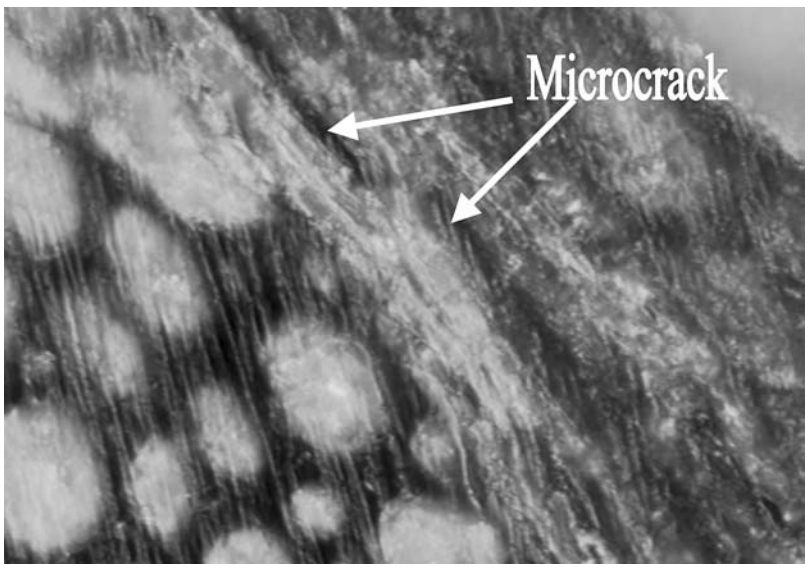

Figure 11 Observed microcrack in the hardwood corresponding to experimental data in Fig. 9

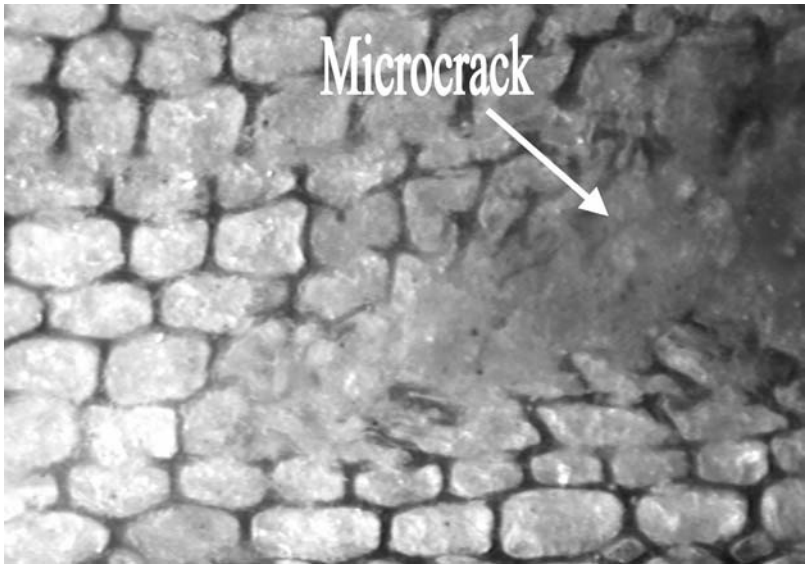

Figure 12 Observed microcrack and cell deformation in the softwood corresponding to experimental data in Fig. 10. The blurring at the microcrack is caused by adherence of dust resulting from sanding the test piece.

a mixture of Mode II_{RL}, III_{RT} and III_{TR} or II_{TL}, III_{TR} and III_{RT} depending on whether the *TL* or *RL* planes, respectively, are perpendicular to the twist axis. Fig. 13 shows a hardwood test-piece with the *RL* plane perpendicular to the twist axis. Fig. 14 shows a diagram of the combined cracking modes for this orientation and indicates that the fracture mode for this test-piece is a mixture of the modes II_{TL}, III_{TR} and III_{RT}. For torsional shear loading Mode I produces fewer AE counts than Modes II and III which suggests that crack initiation in Mode I, or where Mode I is a significant proportion in mixed mode fracture, is easier [16].

The ratio of load at the onset of AE to maximum load, given in Table I, is generally higher for the softwood test-pieces compared with the hardwood. An exception to this is for softwood with a 90° grain angle, where this ratio is lower than that for hardwood. This suggests that for grain angles at 0° or 45°, there is more elastic strain energy stored in the softwood test-pieces prior to crack nucleation than in the hardwood test-pieces. When a crack nucleates, the available energy for driving crack growth is greater in softwoods, so that sudden fracture occurs. A comparison of the hardwood and the softwood with grain angles of 0° and 45° shows that hardwoods produce far more acoustic emission counts than softwoods during static torsion fracture. The ratios of the load at the onset of AE to maximum load for the hardwood are also less than those for the softwood. This means that

TABLE I Acoustic activities for static torsional experiments for samples with different grain orientations. All tests were performed at the same angular twist rate. Module 303 has been used

Type of wood	Grain angle	Torsional shear stress at the onset of AE (MPa)	Ultimate torsional shear stress (MPa)	Load at AE onset Maximum load	Total AE counts up to ultimate load	Number of samples tested
Hardwood	0°	3.81 ± 0.50	13.45 ± 1.0	0.28	5499 ± 3649	5
	9°	1.13	7.45	0.15	4110	1
	45°	1.03 ± 0.40	4.47 ± 0.60	0.23	877 ± 184	3
	90°	0.34 ± 0.50	1.61 ± 0.50	0.21	2705 ± 1605	3
Softwood	0°	10.28 ± 0.50	12.30 ± 0.50	0.84	482 ± 182	4
	35°	3.02	6.69	0.45	1710	1
	45°	1.67	3.35	0.50	196	1
	90°	0.27 ± 0.20	2.16 ± 0.50	0.13	2725 ± 1755	3

TABLE II The relationship between grain angle and fracture mode of wood under torsional loading [19]

Type of wood	Hardwood			Softwood		
Grain angle	0°	45°	90°	0°	45°	90°
Fracture modess	II_{RL} and III_{RT}	I_{RL} and I_{RT}	II_{RL}, III_{RT} and III_{TR} or II_{TL}, III_{TR} and III_{RT}	II_{TL} and III_{TR}	I_{TL} and I_{TR}	II_{TL}, III_{TR} and III_{RT} or II_{RL}, III_{RT} and III_{TR}

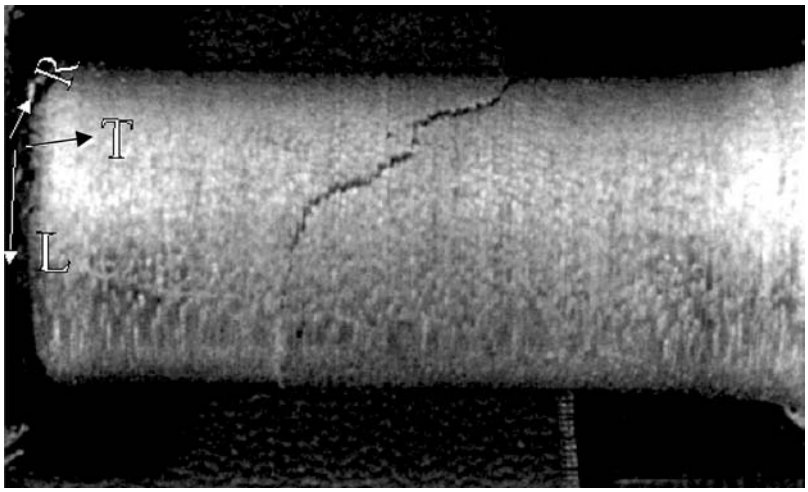

Figure 13 A hardwood sample with the LR plane perpendicular to the twist axis (grain angle is 90°).

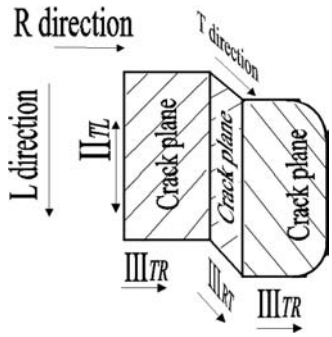

Figure 14 Combined cracking mode in a hardwood with the LR plane perpendicular to the twist axis (grain angle is 90°).

cracking in the hardwood takes place in the earlier stages of loading and continues more gradually than in the softwood, if their grain orientations are between 0° and 45°. The ratio of load at AE onset to maximum load for the hardwood also approximates to that of the softwood. One of the hardwood pieces having a 0° grain angle had the highest total AE counts at maximum loading. This means that this hardwood sample, having a 0° grain angle, produces more AE counts than others during cracking.

The difference in slope in the total AE counts versus time curve before and after the maximum shear stress in hardwood with a 0° grain angle (Fig. 3) could be the result of microcrack formation followed by crack propagation. This behaviour has been reported by Reiterer *et al*. [16]. For some samples, such as those with a 45° grain angle, there are no acoustic emission counts during crack propagation because samples failed catastrophically. It is interesting to note the differences in fracture behaviour found in this study and the Mode I fracture in hardwood and softwood under tensile loading reported by Reiterer *et al*. [16]. In the latter work AE events began in the range 75% to 95% of maximum force. There was little difference in the onset of AE activity between softwood and hardwood, but softwood produced more total AE events than hardwood. Furthermore, there was more reported activity before macrocrack formation for softwoods. Under torsional loading AE events began in the range 13% to 84% for different grain orientations, hardwood produced more total AE counts than softwood and final fracture in the softwood was sudden compared with the gradual process in the hardwood. A possible reason is that the hardwood has a more complicated structure than that of the softwood [19].

3.2. Cyclic torsional test monitoring using acoustic emission

3.2.1. Acoustic emission for each cycle

Fatigue tests were carried out on softwood and hardwood test-pieces, and AE events at each stage of a test were recorded. Kánnár's definition, that the Kaiser effect is accepted when the AE events obtained during the second and later loading cycles are fewer than 50% of those in the first loading cycle, was used when measuring the Kaiser effect [17]. Table III shows the AE events for each loading cycle at an early testing stage and at the failure stage during fatigue testing for hardwood and softwood with a 0°grain angle. It can be seen that before fatigue failure takes place, AE events in most of the later loading cycles do not exceed the AE events in the first cycle. It can therefore be acknowledged that there is little acoustic activity in these cycles of loading in agreement with the Kaiser effect. In the second loading cycle and 156th loading cycle during fatigue testing of a hardwood, AE events are equal to the AE events in the first loading cycle and this suggests that there is microcracking occurring. When fatigue failure begins, AE events surpass the AE events in the first loading cycle and will be surpassed by AE events in later loading cycles if more cracking takes place later. This is illustrated, for example, by the data in Table III for cycles 161–164 in the hardwood and cycles 4–10 in the softwood. So microcrack initiation and then crack initiation and propagation can be determined and

TABLE III AE events taking place at different stages of torsional cyclic loading. Module 920 has been used

Type of wood	Twist angle	Cycle number	AE events	Extistence of Kaiser effect +yes/−no
Hardwood	11.1°	1	332	
		2	338	–
		3	173	–
		4	58	+
		5	139	+
		6	62	+
		7	18	+
		8	64	+
		9	13	+
		10	60	+
		156	324	–
		157	160	+
		158	148	+
		159	172	+
		160 (cracks appearing)	469	–
		161	433	–
		162	256	–
		163	403	–
		164	342	–
		165	9	+
Softwood	11.1°	1	183	
		2	30	+
		3	49	+
		4 (cracks appearing)	405	–
		5	491	–
		6	487	–
		7	225	+
		8	485	–
		9	391	+
		10	315	+

distinguished by the level of AE events before and after cracking takes place.

3.2.2. Acoustic Emission total counts versus cycle number

In order to compare the maximum shear stress and the total AE counts at each loading cycle, plots of these parameters versus cycle number are shown in Figs 15–17. Both the hardwood and softwood samples were tested using displacement control with a twist angle of 11.1°. In the data for load versus cycle number, the point at which the maximum load begins to drop drastically corresponds to the cycle where total or partial fracture takes place. Figs 15 and 16 show that at the point of fracture, the total AE counts start to increase faster than before. So the rate of total AE counts reflects a partial or total fatigue fracture. Figs 15 and 16 also show that the maximum load for each cycle decreases progressively prior to the fracture point. This indicates that there are relaxation phenomena taking place during the torsional fatigue of wood. Prior to this the total AE counts generally increase before crack propagation.

The fatigue test on the hardwood (Fig. 15) also shows that crack propagation will convert some of the elastic energy to acoustic and other forms of energy, as indicated by the partial drop in load, but not all. So the rate of total AE counts increases rapidly following crack propagation and then reduces. This will be repeated if another crack forms. These results show that fractures in hardwood form progressively. The fracture characteristics in wood depend on microstructure and in particular on cell size and cell wall thickness. In a hardwood the cell density is greater than in softwood and therefore cracks have to overcome more obstructions during propagation compared with softwood. Therefore cyclic damage in hardwood is gradual with crack growth along the longitude and tangential direction. In softwood, the thinner earlywood cell walls deform and fail more easily and therefore more quickly and completely so that sudden crack propagation occurs in the longitude and radial direction. These observations are also revealed in the hysteresis loops during both static and fatigue loading of hardwood and softwood. For the hardwood the hysteresis loops can still be observed after cracking has commenced, showing that a hardwood dissipates energy after cracking occurs. This is reflected in the greater number of AE counts in the hardwood compared with softwood before cracking. For the softwood the loops decreased in area with each loading cycle and disappeared in the few cycles prior to failure [19].

A comparison of the total AE counts for hardwood and softwood shows that hardwood generates more total AE counts than softwood at the cycle just before a sudden load decrease at failure (Fig. 17). As reported earlier this is different to Reiterer *et al.*'s finding for testing done under tensile loading and Mode I crack opening [16]. Reiterer suggests that softwood generates more total AE counts than hardwood at the fracture cycle. Fig. 17 shows that there is a total AE increase in hardwood at a much earlier stage before the maximum load attained in each cycle begins to drop. Compared with hardwood, the total AE increase in softwood takes place later, more slowly and at a lower level before the maximum load attained in each cycle begins to drop.

The increase in total AE at the fracture point in softwood is larger than that found in hardwood under cyclic torsional loading (Fig. 17). This result seems to agree with results from static torsional work, where softwood samples with a 0° grain angle have a higher torsional stress at the onset of AE than hardwood with a 0° grain angle, although the latter has a higher ultimate torsional stress (Table I). Both results indicate that the manner of fracture in softwood is sudden and complete, and the fracture mode in hardwood is slow and progressive.

3.3. Comparison of total AE counts in cyclic testing with that in static testing

Table IV compares the total AE counts at the onset of fracture for test-pieces under cyclic torsion with those tested

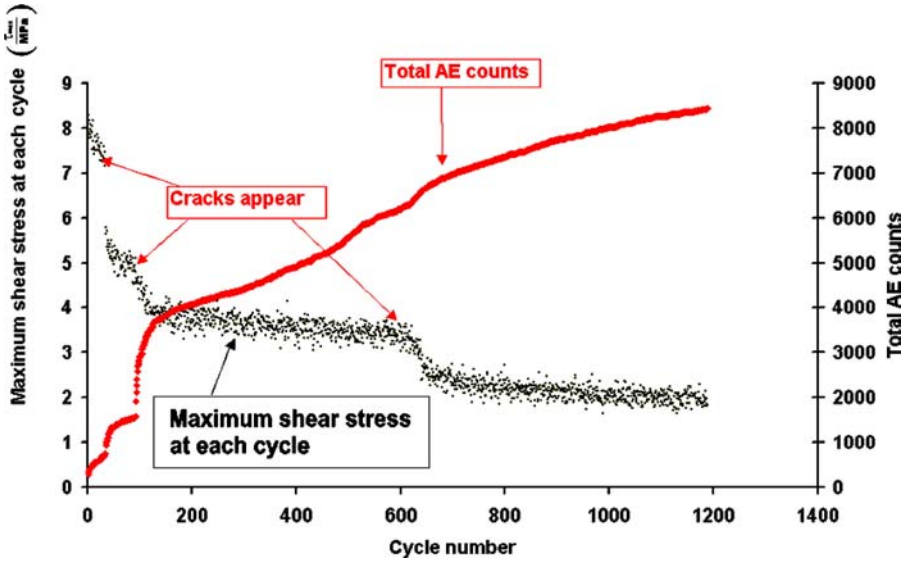

Figure 15 AE counts-cycle curve compared with loading-cycle curve for the hardwood. The twist angle was controlled at 11.1°. Module 303 has been used.

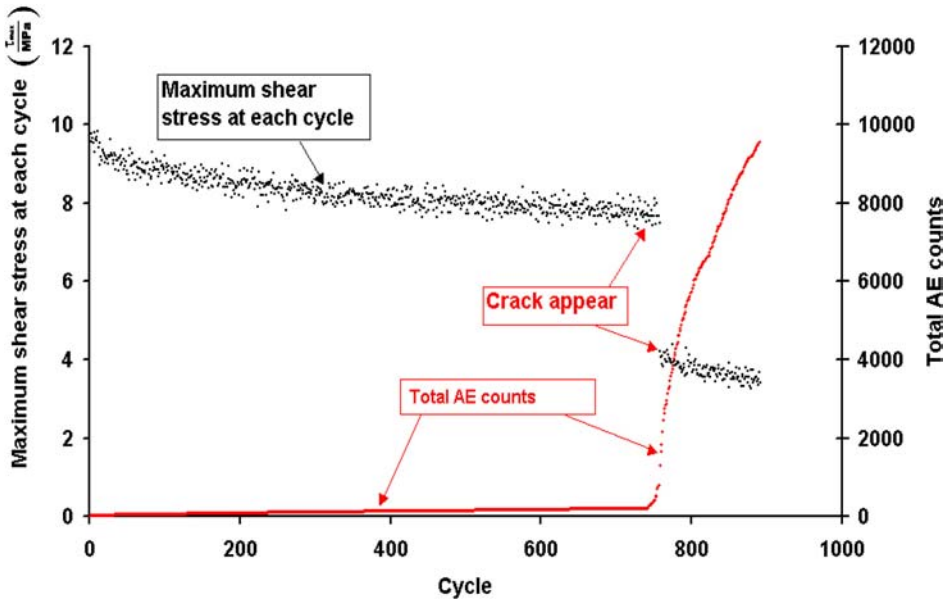

Figure 16 AE counts-cycle curve compared with loading-cycle curve for the softwood. The twist angle was controlled at 11.1°. Module 303 has been used.

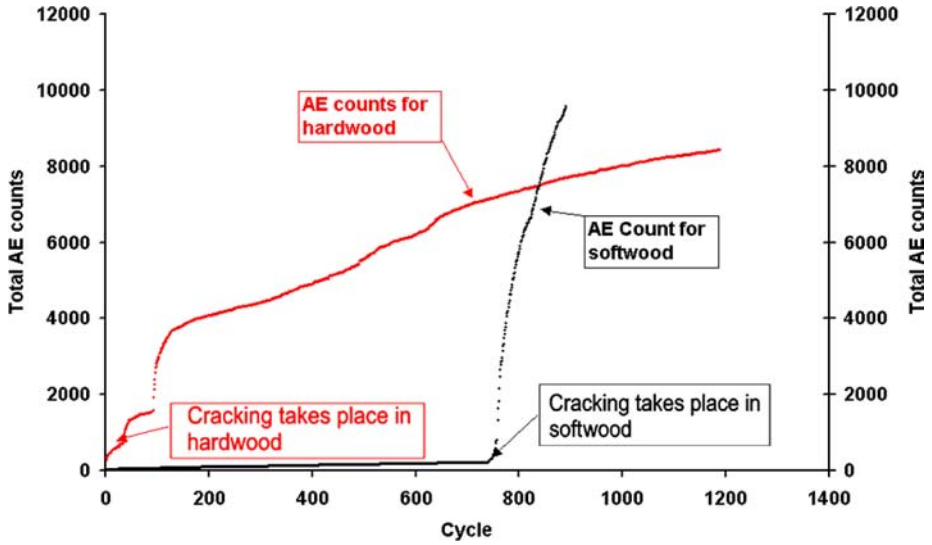

Figure 17 AE total counts-cycle curve for a hardwood compared with that for a softwood. Module 303 has been used.

TABLE IV Acoustic activities at fracture for samples under static torsional loading and cyclic torsional loading. Each test has been repeated 4 times. Module 303 has been used

Sample	Angle of twist	Increase of total AE count at onset of crack propagation
Hardwood		
Static	20.0°	3380
Cyclic	11.1°	6954
Cyclic	6.8°	3373
Softwood		
Static	14.9°	2860
Cyclic	11.1.0°	8135
Cyclic	6.4°	808

in static torsion. For comparison all samples have a 0° grain angle and the fatigue samples were tested at several twist angles. The results show that in general the fatigue samples produced more total AE counts than the statically tested samples if the angle of twist is large enough. In cyclic torsional testing, as the twist angle is reduced, the hardwood gives almost the same total AE counts as in a static test and the softwood gives fewer total AE counts compared with the static test. A possible explanation is that there is more internal friction in fatigue fracture than in static fracture before cracking occurs if the twist angle is sufficiently large. This would derive from reversed cell wall deformation and relative movement of crack faces. This leads to greater energy release from fatigue test-pieces than static test-pieces at such a level of twist angle. If the twist angle during fatigue is smaller than a certain level, during the fracture process there is less internal friction and less energy to be released than in the static test-pieces.

4. Conclusion

1. In static torsional testing, the acoustic activity prior to maximum load indicates that some microcrack initiation is taking place prior to visible cracking in both hardwood and softwood. This is supported by microscopic observations.

2. Under torsional loading, the test-piece grain angle influences the total AE counts up to the fracture. AE counts decrease as the grain angle increases from 0° to 45° and increases as the grain angle increases from 45° to 90°. The softwood samples with a 45° grain angle have the smallest increase in total AE counts. The hardwood produced more AE counts than the softwood for 0° and 90°.grain angles.

3. In fatigue testing, the results from acoustic emission measurements indicate some micro-crack initiation in hardwood and softwood during torsional fatigue testing. Hardwood has more total AE counts than softwood before the onset of cracking, but softwood has a higher total AE count than hardwood after cracking has taken place. The results also indicate that both hardwood and softwood show the Kaiser effect in some torsional loading cycles before cracking.

4. Provided the angle of twist is larger than a certain minimum value, fatigue samples produce more total AE counts during fracture than static samples.

5. For softwoods, with grain parallel to the twist axis, the higher ratio of load at the onset of AE to maximum load, when tested in static torsion and the higher rate of increase in total AE at fracture in cyclic torsion, suggests that fracture in softwood is more sudden and complete under both static and cyclic torsional loading compared with hardwood.

6. The results show that it is possible to monitor and analyze the failure process in wood when under torsional loading using acoustic emission techniques.

Acknowledgments

The authors wish to thank Dr P.Bonfield, of the Building Research Establishment(UK), for supplying the Sitka spruce used in this work.

References

1. R. G. LIPTAI, D. O. HARRIS and C. A. TATRO, in "Astm-Stp" **505** (1972).
2. A. E. LORD JR., *Phys. Acousti.* **15** (1983) 295.
3. R. W. NICHOLS, in "*Acoustic Emission*" (Applied Science, London, UK, 1976).
4. L. C. LYNNWORTH, in "Ultrasonic Measurements for Process Control, Theory, Techniques, Applications" (Academic Press, New York, USA, 1989).
5. R. B. STEPHENS and H. C. LEVINTHALL, in "Acoustics and Vibration Progress " (Chapman & Hall, London, UK, 1974).
6. R. V. WILLIAMS, in "Acoustic Emission " (Adam Hilger Ltd., Bristol, England, 1980).
7. V. BUCUR, in "Acoustics of Wood " (CRC Press, Boca Raton, New York, USA, 1995) 221.
8. S. L. QUARLES, *Wood Fibre Sci.* **24** (1992) 2.
9. I. D. BOOKER, *Holz Roh-Werkstoff* **52** (1994a) 383.
10. J. D. BOOK, *Wood Sci. and Tech.* **28** (1994b) 249.
11. S. J. KOWALSKI, W. MOLIŃSKI and G. MUSIELAK, *ibid.* **38** (2004) 35.
12. M. P. ANSELL, *ibid.* **16** (1982) 35.
13. A. P. SCHNIEWIND, S. L. QUARLES and H. LEE, *ibid.* **30** (1996) 273.

Received 16 May
and accepted 19 August 2005